Preparation and characterization of high-strength low-thermal-conductivity cement-based insulation materials

IOP Conf. Series: Materials Science and Engineering **542** (2019) 012070 doi:10.1088/1757-899X/542/1/012070

Preparation and characterization of high-strength low-thermal-conductivity cement-based insulation materials

X X Zhang, Z P Wang*, A M She, Y Q Wei and Z Y Zhu

Key Laboratory of Advanced Civil Engineering Materials of Ministry of Education, Tongji University, Shanghai, China
E-mail: zxxlucky@126.com

Abstract. Thermal insulation materials with high strength and ultra-low thermal conductivity are ideal construction ones for residential infrastructure. However, high strength of materials regularly means high thermal conductivity. To solve this problem, a novel thermal insulation material was prepared by using cement as the binder, silica fume as the mineral admixture, aerogel as the coarse filler and hollow SiO_2 microsphere as the fine filler. The optimal proportion and preparation process were investigated by means of the orthogonal experiment and the single factor experiment method, respectively. On the other hand, their microstructures, in terms of aerogel particle size distribution and multi-scale composite structure were analysed by optical microscope, binarization image, scanning electron microscope. The results indicated that compared to conventional insulation materials, the produced materials in this study behaved much better performance in strength. The dry density, compressive strength and thermal conductivity reached 360 kg/m^3, 4.55 MPa and 0.055 W/m·K, respectively. The incorporation of hollow SiO_2 microsphere and silica fume led to the much thicker pore walls of the sample, and simultaneously the prolonging of stirring time resulted in the much smaller size of aerogel, which were considered as the two primary causes of its excellent mechanical performance.

1. Introduction

Lightweight cement-based insulation materials are manufactured by introducing lightweight fillers or foam into cement. Because of their advantages of superior durability, fire-resistant and safety, they are extensively used in thermal insulation projects[1, 2]. In lightweight cement-based insulation materials, low thermal conductivity depends on high porosity and low density, but high strength depends on low porosity and high density[3-5]. Therefore, it is difficult to prepare a cement-based insulation material with low dry density, low thermal conductivity, and high strength[6, 7]. The pore and pore wall structure are the main factors affecting compressive strength and thermal conductivity[8, 9]. Studies have shown that under the same porosity, small and uniform pore is beneficial to increase compressive strength[5]. The pore structure can be controlled by increasing the viscosity of the slurry[10], prolonging the stirring time, and accelerating the stirring rate. In addition, thick and compact pore wall can improve the mechanical properties of the insulation materials. Thick pore walls can be obtained by filling smaller high strength hollow particles between larger ones[11]. Compact pore walls can be developed by using high strength cement, low w/c ratio and large dosage of mineral admixture[12]. As a mineral admixture, silica fume is usually used in cement-based insulation materials in an amount of 5% to 20%, which has the function of assisting gelation and filling fine pores[13-18]. Aerogel has a significant reduction effect on thermal conductivity of thermal insulation mortar[19, 20]. Hollow SiO_2 microsphere has lightweight and high strength characteristic properties in thermal insulation

mortar[21-25]. In this study, cement-based insulation materials with low dry density, low thermal conductivity and high-strength were prepared. Silica fume (content >60%) was used as mineral admixture, aerogel and hollow SiO_2 microspheres were used as porous lightweight fillers. An ultra-low w/c ratio was chosen to improve compressive strength. The effects of raw material composition and stirring time on the properties of thermal insulation materials were analysed, and the relationship between microscope morphology and macroscopic properties was studied.

2. Materials and methods

2.1. Materials and preparation

PII 52.5 cement: average particle size was 18 μm. Silica fume: average particle size was 0.3 μm. Hollow SiO_2 microspheres: average particle size was 25 μm, bulk density was 250 kg/m^3, compressive strength was 80 MPa, thermal conductivity was 0.05 W/m·K. Aerogel: average particle size was 2090 μm, bulk density was 75 kg/m^3, thermal conductivity was 0.02 W/m·K. Superplasticizer: water reduction rate was 28%, dosage was 5% (by cement mass). The raw materials particle size distribution and microscope morphology were shown in figure 1 and figure 2.

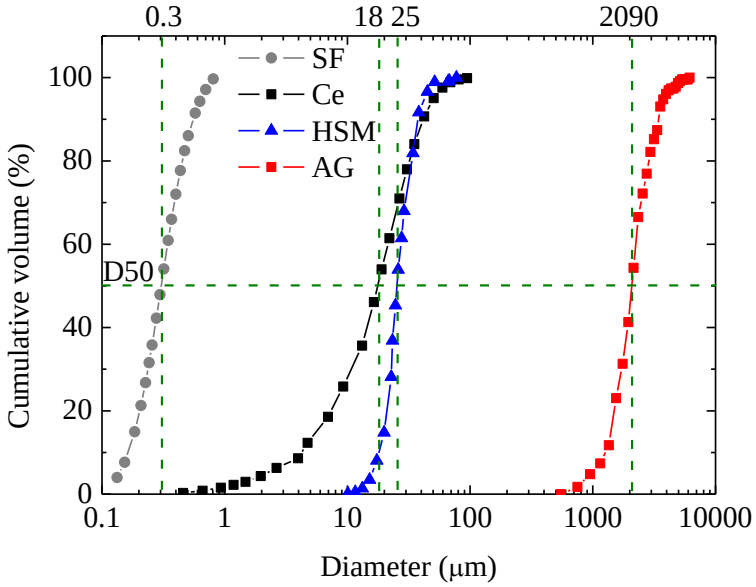

Figure 1. Particle size distributions of raw materials with Ce=cement, SF=silica fume, HSM=hollow SiO_2 microsphere, AG=aerogel.

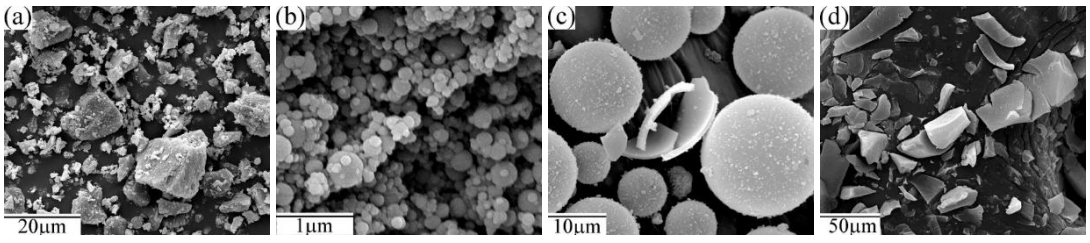

Figure 2. Microscope morphology of raw materials with (a) Ce, (b) SF, (c) HSM, (d) AG.

2.2. Test methods

2.2.1. Sample preparation. Cement, silica fume and pre-wet hollow SiO_2 microspheres were added to the stirring pot for dry mixing for 30 s. Water (containing superplasticizer) was added to the dry mixture for stirring slowly for 60 s, and stirring quickly for 60 s. The aerogel was added to the slurry and stirred quickly for the corresponding time. The prepared slurry was poured in a mold and covered

with a plastic film. After 48 h, specimens were released from the molds and cured at 20±2 °C and 75% RH for 28d.

The optimal recipe was explored by orthogonal experiment. The factors and levels of the orthogonal experiment were shown in table 1. The stirring time after the addition of the aerogel in the orthogonal experiment was 90 s.

Table 1. Orthogonal experimental factor and level.

Level	A SF/Ce /(wt.[a])	B HSM/Ce /(wt.[a])	C AG/Ce /(wt.[a])	D W[b]/Ce /(wt.[a])
1	0.6	1.25	0.45	2.18
2	1	1.75	0.6	2.26
3	1.4	2.25	0.75	2.34

[a] Weight.
[b] Water.

2.2.2. Performance Testing. Dry density, compressive strength and thermal conductivity of samples were tested according to Chinese national standard GB/T5486-2008, GB/T5486-2008 and GB/T10294-2008, respectively. The aerogel in the thermal insulation materials was analysed by MF-UA1010D optical microscope. The microscope morphology of the thermal insulation materials was analysed by Quanta 200F scanning electron microscope (SEM).

3. Results and discussion

3.1. Effect of raw material composition on macroscopic performance

The orthogonal test results and analysis of the cement-based insulation materials were shown in table 2 and table 3. It can be seen from table 3 that the optimal recipe under the dry density index was $A_1B_1C_3D_3$, and the main factors affecting the dry density were successively: aerogel> silica fume> water> hollow SiO_2 microspheres. The optimal recipe under the compressive strength index was $A_1B_3C_1D_1$, and the main factors affecting compressive strength were successively: silica fume> aerogel> water> hollow SiO_2 microspheres. The optimal recipe under the thermal conductivity index was $A_1B_1C_3D_3$, and the main factors affecting thermal conductivity were successively: aerogel> silica fume> water> hollow SiO_2 microspheres.

Table 2. Orthogonal experimental results of cement-based insulations.

Sample No.	ρ[a] /(kg/m^3)	f_{28d}[b] /MPa	λ[c] /(W/m K)	f_{28d}/λ[d] /(MPa/(W/m K))
1	408	4.44	0.105	42.29
2	359	3.72	0.064	58.13
3	324	3.09	0.051	60.59
4	343	1.03	0.057	18.07
5	346	1.69	0.058	29.14
6	412	2.75	0.112	24.55
7	355	1.47	0.061	24.10
8	414	2.16	0.113	19.12
9	396	2.22	0.088	25.23

[a] Dry density.
[b] 28d compressive strength.
[c] Thermal conductivity.
[d] The ratio of 28d compressive strength to thermal conductivity.

Table 3. Orthogonal experimental analysis of cement-based insulations.

Effect	k_1[a]	k_2[a]	k_3[a]	R[b]	BR[c]
ρ	364	367	388	25	A_1

/(kg/m^3)	369	373	377	9	B_1
	411	366	341	70	C_3
	383	375	360	23	D_3
	3.75	1.82	1.95	1.93	A_1
f_{28d}	2.31	2.52	2.69	0.38	B_3
/MPa	3.11	2.32	2.08	1.03	C_1
	2.78	2.65	2.09	0.69	D_1
	0.073	0.076	0.087	0.014	A_1
λ	0.074	0.078	0.084	0.009	B_1
/(W/m K)	0.110	0.070	0.057	0.053	C_3
	0.084	0.079	0.074	0.010	D_3

[a] k_i=the average value of i level in three experiments.
[b] Range.
[c] The best result.

The effect of the composition of the raw materials on the properties of the insulation materials was shown in figure 3. It can be seen from figure 3 that SF/Ce, HSM/Ce, AG/Ce and W/Ce had an important influence on the properties of the insulation materials. With the SF/Ce value increasing, the dry density and thermal conductivity of the thermal insulation materials increased, and the compressive strength firstly decreased and then increased. As the HSM/Ce value increased, the dry density, compressive strength and thermal conductivity of the insulation materials all increased slightly. Compared to other three factors, the factor of HSM/Ce had the minimum ranges: 9 kg/m^3, 0.38 MPa and 0.009 W/m K. The possible reason was that the compressive strength and thermal conductivity of the hollow SiO_2 microspheres were similar to those of the prepared thermal insulation materials. The dry density, compressive strength and thermal conductivity all decreased greatly with the AG/Ce value increasing, which was due to the ultra-high porosity of aerogel. As the W/Ce value increased, the dry density, compressive strength, and thermal conductivity of the insulation materials all decreased.

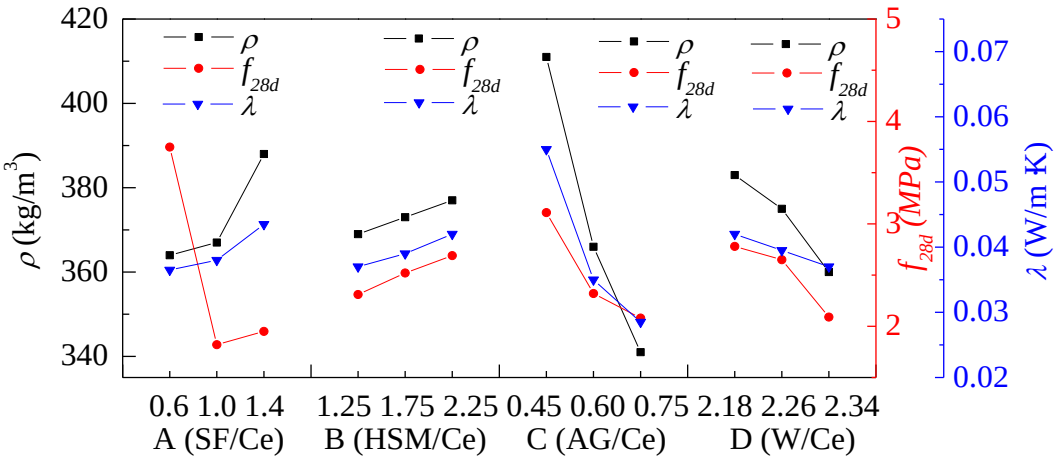

Figure 3. Effect of SF/Ce, HSM/Ce, AG/Ce, W/Ce on properties of thermal insulation materials.

The recipe and results of the optimal ratio under single index condition were shown in table 4. It can be seen from table 4 that the optimal recipe under different index had different properties. In order to obtain high-strength and low-thermal-conductivity insulation materials, the ratio of compressive strength to thermal conductivity (f_{28d}/λ) was introduced and used as an evaluation index. The f_{28d}/λ value reflects the compressive strength per unit of thermal insulation capacity. The f_{28d}/λ values in table 3 and table 4 ranged from 18.07 to 60.59 MPa/(W/m K), among which the f_{28d}/λ value of sample No.3 was highest, being 60.59 MPa/(W/m K). By Considering various factors, sample No.3 with the

highest f_{28d}/λ value was the optimal ratio, being $A_1B_3C_3D_3$. The dry density was 320 kg/m^3, the compressive strength was 3.09 MPa and the thermal conductivity was 0.051 W/m K.

Table 4. Optimal recipe and its results under single index condition.

Sample No.	A SF/Ce	B HSM/Ce	C AG/Ce	D W/Ce	Performance			
					ρ /(kg/m^3)	f_{28d} /MPa	λ /(W/m K)	f_{28d}/λ /(MPa/(W/m K))
$A_1B_1C_3D_3$	0.6	1.25	0.75	1.21	297	1.52	0.048	31.67
$A_1B_3C_1D_1$	0.6	2.25	0.45	1.08	418	4.52	0.125	36.16
$A_1B_1C_3D_3$	0.6	1.25	0.75	1.21	297	1.52	0.048	31.67
3	0.6	2.25	0.75	1.21	324	3.09	0.051	60.59

3.2. Effect of stirring time on macroscopic performance

Using sample No.3, the effect of stirring time after the addition of aerogel on the performance of thermal insulation materials was studied, and the test results were shown in figure 4. As can be seen from figure 4, the dry density, compressive strength, thermal conductivity, and f_{28d}/λ value of the thermal insulation materials all increased with stirring time increasing. When the stirring time extended from 30 s to 120 s, the dry density varied from 277 kg/m^3 to 360 kg/m^3, increased by 30%; the compressive strength varied from 1.12 MPa to 4.55 MPa, increased by 300%; the thermal conductivity varied from 0.042 W/m K to 0.055 W/m K, increased by 31%; and the f_{28d}/λ value varied from 26.67 MPa/(W/m K) to 82.73 MPa/(W/m K), increased by 210%. It can be seen that as the stirring time increased, the dry density and thermal conductivity increased slightly, while the compressive strength and the f_{28d}/λ value increased significantly. In other words, prolonging stirring time was an effective method to improve compressive strength under the premise of ensuring low thermal conductivity. When the stirring time was 120 s, the thermal insulation materials had the highest f_{28d}/λ value. The dry density was 360 kg/m^3, the thermal conductivity was 0.055 W/m K, and the compressive strength was 4.55 MPa.

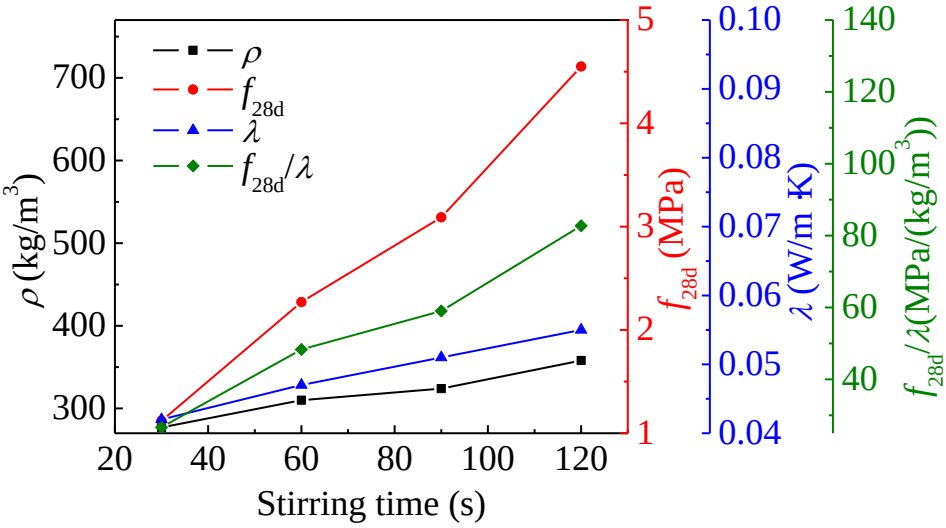

Figure 4. Effect of stirring time after adding AG on properties of thermal insulation materials.

3.3. Microstructure

The average particle size of the aerogel and hollow SiO_2 microspheres used in the work were 2090 μm and 25 μm. In order to investigate the distribution of porous lightweight fillers under different scales in the thermal insulation materials, optical microscope and SEM analyses of thermal insulation materials cross-section were carried out.

3.3.1. Aerogel morphology and particle size distribution in thermal insulation materials. The optical micrograph of the thermal insulation materials cross-section was binarized by image software, the pores left by the aerogel and the surrounding matrix were indicated in black and white respectively, as shown in figure 5. The stirring time had an important impact on the size, shape and position distribution of the aerogel particles in the thermal insulation materials. When the stirring time extended from 30s to 120s, the size of the aerogel became smaller, the edge of the aerogel varied from smooth to rough, and the position distribution of aerogel varied from large particles evenly distributing to small particles filling large particles' gap. These three changes were respectively beneficial to reduce stress concentration phenomenon, enhance interfacial adhesion, and improve particle gradation, thereby increasing the compressive strength.

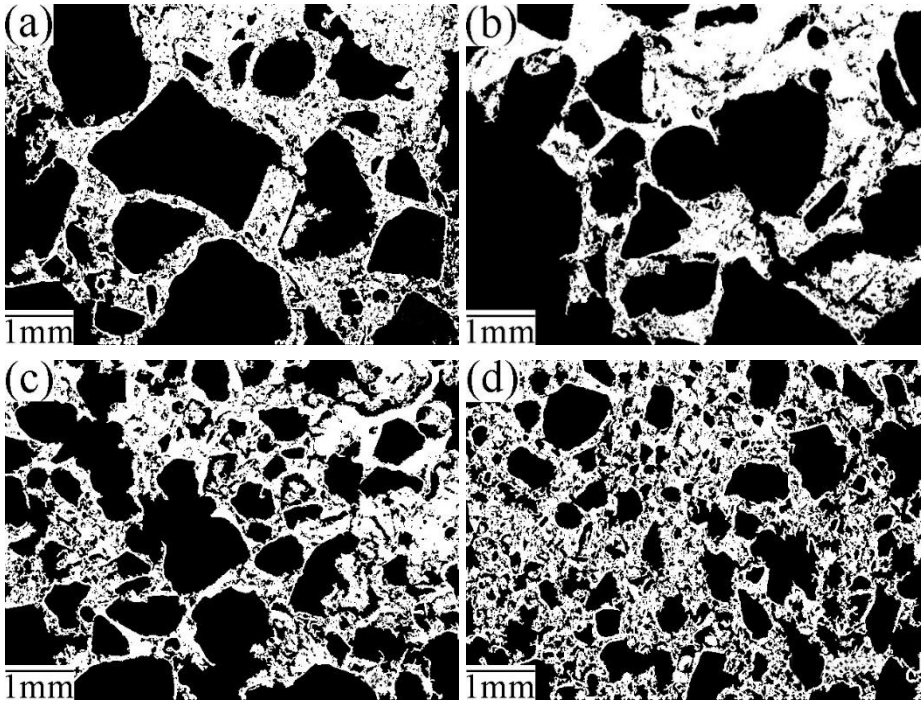

Figure 5. Binary graph of insulation materials cross-section with (a) stirring 30s, (b) stirring 60s, (c) stirring 90s, (d) stirring 120s.

The particle size analysis software was used to obtain the aerogel particle size, and its distribution was plotted as shown in figure 6. The stirring time had an important influence on the particle size distribution of the aerogel. When the stirring time extended from 30 s to 120 s, the average particle size of aerogel was reduced from 0.67 mm to 0.21 mm with a decrease of 69%, and the particle size distribution was changed from 45% of 0-0.6 mm, 38% of 0.6-1.2 mm, 17% of 1.2-1.8 mm, to 93% of 0-0.6 mm, 7% of 0.6-1.2 mm, 0% of 1.2-1.8mm. Among them, the particle numbers at size of 0~0.6 mm was increased by 48%, those at size of 0.6-1.2 mm and 1.2-1.8 mm were decreased by 31% and 17% respectively. The particle size distribution of aerogel concentrated to 0-0.6 mm. When the stirring time extended from 30 s to 120 s, the f_{28d}/λ value of the insulation materials increased from 26.67 MPa/(W/m·K) to 82.73 MPa/(W/m·K). It can be seen that prolonging stirring time made the aerogel particle size smaller, and the distribution gathers towards 0-0.6 mm, which eventually led to an increase of f_{28d}/λ value.

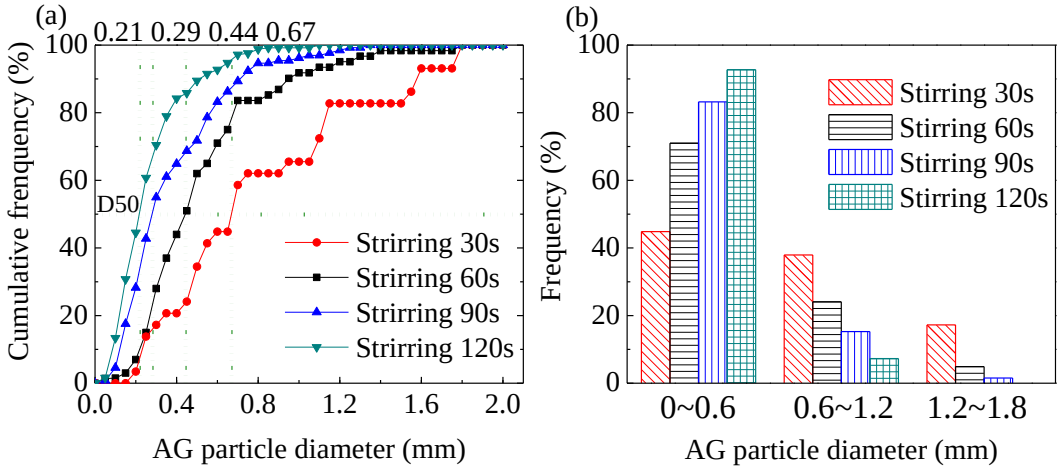

Figure 6. Aerogel particle size distribution in thermal insulation materials with (a) cumulative frequency distributions and (b) frequency distributions.

3.3.2. Cross-section microstructure. The SEM images of the cross-section of the thermal insulation materials were shown in figure 7(a). Figure 7(b), (c), and (d) were enlarged images of the square boxes in figure 7(a), (b), and (c), respectively.

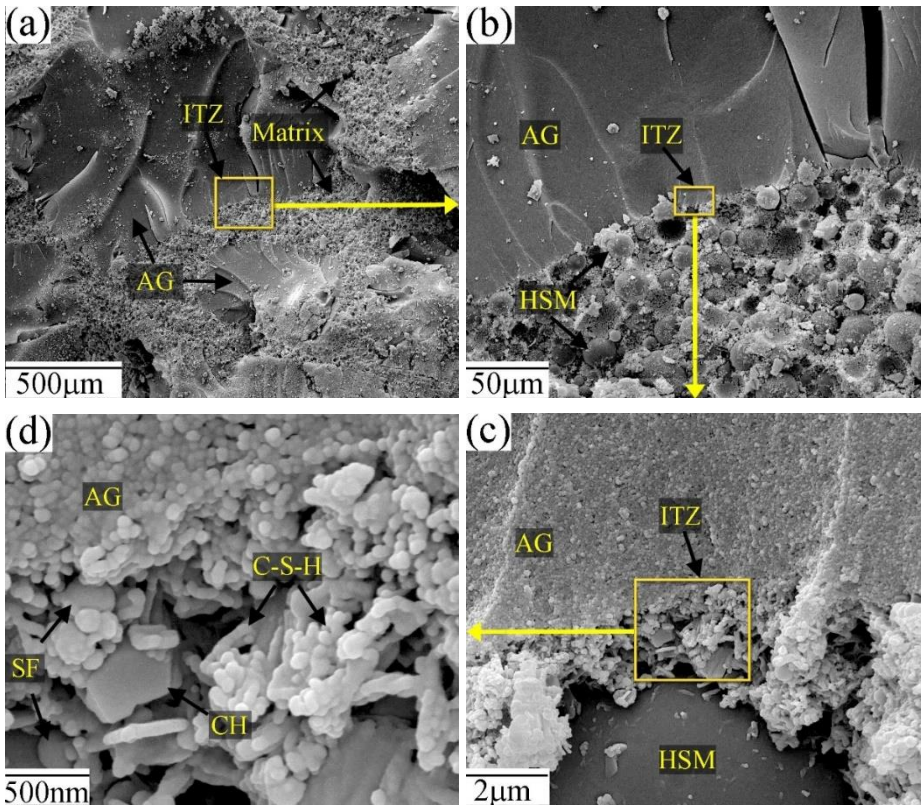

Figure 7. Multi-scale microstructure of thermal insulation materials.

As can be seen from figure 7(a), the aerogel (AG, smooth surface) distributed evenly in the matrix (Matrix, rough surface), and the interfacial transition zone (ITZ) of aerogel and matrix had no macroscopic crack and was linked tightly and closely. This may be one of the reasons for the high mechanical properties of thermal insulation materials. Combining figure 7(b) and (c), it can be seen that the matrix consisted of hollow SiO_2 microspheres (HSM) and cement hydration products, and the hollow SiO_2 microspheres were embedded in the hydration products tightly. Aerogels can be regarded as pores because of their high porosity, and matrix composed of hollow SiO_2 microspheres and

hydration product can be viewed as compact pore wall (i.e. bubble spacing). Studies have shown that filling large pore gaps with small fillers can widen the bubble spacing and thicken the pore walls, thus increasing the compressive strength[11]. It can be reasonably assumed that the presence of the hollow SiO_2 microspheres herein increased the distance between the aerogels, thickened the pore walls, thereby improving the mechanical properties of the thermal insulation materials. It can be seen from figure 7(d) that the cement hydration products were mainly cigar-like C-S-H gels and micro-nano scale $Ca(OH)_2$ crystals; unhydrated silica fume particles presented in the interval of hydrated products. C-S-H gels were the main source of cement stone strength, smaller size $Ca(OH)_2$ crystals were beneficial to reduce the loss of strength, and unhydrated silica fume particles filling micro-nano pores was beneficial to improve the compactness of the pore walls. These three aspects reasons on the micro-nano scale led to better mechanical properties of the thermal insulation materials. The C-S-H gels bonded different sizes of aerogel and hollow SiO_2 microspheres to form a multi-scale microstructure: the aerogel and hollow SiO_2 microspheres particle size mainly distributed around 210m and 25m, despite the particle size distribution of overall was wide, that of each scale was concentrated. A good particle gradation was obtained by controlling particle size distribution, then a lightweight and high-strength insulation material could be achieved.

4. Conclusions

In this study, the effect of raw materials composition and stirring processing on the properties of cement-based thermal insulation materials was investigated. The microstructure of the thermal insulation materials was analysed. The results can be summarized as follows:

(1) The optimal material ratio obtained by orthogonal experiment was cement: silica fume: hollow SiO_2 microsphere: aerogel: superplasticizer: water = 1:0.6:2.25:0.75:0.05:2.34. The main factors affecting dry density, compressive strength and thermal conductivity were successively aerogel, silica fume and water content. The optimal stirring time after adding the aerogel was 120 s. The prepared thermal insulation material had a dry density of 360 kg/m^3, a compressive strength of 4.55 MPa, and a thermal conductivity of 0.055 W/m K.

(2) The stirring time had the positive influence on compressive strength. When the stirring time extended from 30 s to 120 s, the aerogel average size was decreased by 69%, which led to a 300% increase in compressive strength.

(3) The produced thermal insulation material consisted of aerogel, hollow SiO_2 microspheres, cement hydration products, and unhydrated silica fume. The hydration product bonded porous fillers with different sizes to form a multi-scale microstructure. And by controlling the sizes of different particles, particle gradation could be properly improved.

Acknowledgements

The authors would like to acknowledge the financial support for this study from the National Natural Science Foundation of China (No.51468002) and the National Key Research and Development Program of China (No.2016YFC0700807).

References

[1] Samson G, Phelipot-Mardelé A and Lanos C, 2017 *Mag Concrete Res* **69** 1-16
[2] Aditya L, Mahlia T M I, Rismanchi B, Ng H M, Hasan M H, Metselaar H S C, Muraza O and Aditiya H B, 2017 *Renew Sust Energ Rev* **73** 1352-65
[3] Ramamurthy K, Nambiar E K K and Ranjani G I S, 2009 *Cement Concrete Comp* **31** 388-396
[4] Wei S, Chen Y, Zhang Y and Jones M R, 2013 *Constr Build Mater* **47** 1278-91
[5] Zeng Q, Mao T, Li H and Peng Y, 2018 *Energ Buildings* **174** 97-110
[6] Chen B and Liu N, 2013 *Constr Build Mater* **44** 691-698
[7] Jones M R, Ozlutas K and Li Z, 2017 *Mag Concrete Res* 1-11
[8] Nambiar E K K and Ramamurthy K, 2007 *Cement Concrete Res* **37** 221-230
[9] Kearsley E P and Wainwright P J, 2002 *Cement Concrete Res* **32** 233-239
[10] Jiang J, Lu Z, Niu Y, Li J and Zhang Y, 2016 *Constr Build Mater* **107** 181-190
[11] Shao N N, Liu Z, Xu Y Y, Kong F L and Wang D M, 2015 *Mater Lett* **161** 451-454

[12] Shi C, Wu Z, Xiao J, Wang D, Huang Z and Fang Z, 2015 *Constr Build Mater* **101** 741-751
[13] Nambiar E K K and Ramamurthy K, 2006 *Cement Concrete Comp* **28** 475-480
[14] Nambiar E K K and Ramamurthy K, 2006 *Cement Concrete Comp* **28** 752-760
[15] Reisi M, Dadvar S A and Sharif A, 2017 *Mag Concrete Res* **69** 1-13
[16] Koksal F, Gencel O and Kaya M, 2015 *Constr Build Mater* **88** 175-187
[17] Babu K G and Babu D S, 2003 *Cement Concrete Res* **33** 755-762
[18] Demirboğa R and Gül R, 2003 *Cement Concrete Res* **33** 723-727
[19] Jia G, Li Z, Liu P and Jing Q, 2018 *Journal of Non Crystalline Solids* **482** 192-202
[20] Jia G, Li Z, Liu P and Jing Q, 2017 *Mag Concrete Res* 1-54
[21] Zhang Q and Li V C, 2015 *Cement Concrete Comp* **60** 10-16
[22] Yun T S, Jeong Y J, Han T S and Youm K S, 2013 *Energ Buildings* **61** 125-132
[23] Oreshkin D, Semenov V and Rozovskaya T, 2016 *Procedia Engineering* **153** 638-643
[24] Gao T, Jelle B P, Sandberg L I and Gustavsen A, 2013 *Acs Appl Mater Interfaces* **5** 761
[25] Ruckdeschel P, Kemnitzer T W, Nutz F A, Senker J and Retsch M, 2015 *Nanoscale* **7** 10059-70